



White Matter Abnormalities in Major Depression Biotypes Identified by Diffusion Tensor Imaging

Sugai Liang^{1,2} · Qiang Wang¹ · Xiangzhen Kong³ · Wei Deng^{1,2} · Xiao Yang^{1,2} ·
Xiaojing Li¹ · Zhong Zhang⁴ · Jian Zhang¹ · Chengcheng Zhang¹ ·
Xin-min Li⁵ · Xiaohong Ma¹ · Junming Shao⁴ · Andrew J. Greenshaw⁵ ·
Tao Li^{1,2}

Received: 2 September 2018 / Accepted: 25 February 2019 / Published online: 6 May 2019
© Shanghai Institutes for Biological Sciences, CAS 2019

Abstract Identifying data-driven biotypes of major depressive disorder (MDD) has promise for the clarification of diagnostic heterogeneity. However, few studies have focused on white-matter abnormalities for MDD subtyping. This study included 116 patients with MDD and 118 demographically-matched healthy controls assessed by diffusion tensor imaging and neurocognitive evaluation. Hierarchical clustering was applied to the major fiber tracts, in conjunction with tract-based spatial statistics, to reveal white-matter alterations associated with MDD. Clinical and neurocognitive differences were compared between identified subgroups and healthy controls. With fractional anisotropy extracted from 20 fiber tracts, cluster analysis revealed 3 subgroups based on the patterns of abnormalities. Patients in each subgroup *versus* healthy controls showed a stepwise pattern of white-matter alterations as follows: subgroup 1 (25.9% of patient sample),

widespread white-matter disruption; subgroup 2 (43.1% of patient sample), intermediate and more localized abnormalities in aspects of the corpus callosum and left cingulate; and subgroup 3 (31.0% of patient sample), possible mild alterations, but no statistically significant tract disruption after controlling for family-wise error. The neurocognitive impairment in each subgroup accompanied the white-matter alterations: subgroup 1, deficits in sustained attention and delayed memory; subgroup 2, dysfunction in delayed memory; and subgroup 3, no significant deficits. Three subtypes of white-matter abnormality exist in individuals with major depression, those having widespread abnormalities suffering more neurocognitive impairments, which may provide evidence for parsing the heterogeneity of the disorder and help optimize type-specific treatment approaches.

Keywords Major depressive disorder · Hierarchical clustering · Diffusion tensor imaging · Biotype · Heterogeneity

Electronic supplementary material The online version of this article (<https://doi.org/10.1007/s12264-019-00381-w>) contains supplementary material, which is available to authorized users.

✉ Tao Li
xuntao26@hotmail.com

- ¹ Mental Health Centre, West China Hospital, Sichuan University, Chengdu 610041, China
- ² Huaxi Brain Research Centre, West China Hospital, Sichuan University, Chengdu 610041, China
- ³ Language and Genetics Department, Max Planck Institute for Psycholinguistics, 6525 XD Nijmegen, Netherlands
- ⁴ Big Data Research Center, School of Computer Science and Engineering, University of Electronic Science and Technology of China, Chengdu 611731, China
- ⁵ Department of Psychiatry, University of Alberta, Edmonton T6G 2B7, Canada

Introduction

Major depressive disorder (MDD) is a heterogeneous clinical syndrome characterized by a range of symptoms, including depressed mood, loss of interest or pleasure, and associated symptoms such as feelings of worthlessness and insomnia [1, 2]. The current diagnosis of depression is entirely dependent on the clinical presentation [3]. Distinction of clear and valid symptomatic subtypes of MDD is difficult due to the complex heterogeneity of the disorder [4]. To date, evidence for associations between clinical symptoms and the putative underlying biological substrates of MDD are inconsistent and variable at the individual level [5]. In addition, group comparisons between patients

with MDD and healthy controls may overlook significant functional changes in the brain of the individual patient [6]. Recently, biological subtyping (clustering of individuals with potential biomarkers) has been recognized as a promising approach for elucidation of the heterogeneity of depression [7]. Unlike the conventional diagnostic categories, the biological subtypes (i.e., biotypes) of depression bridge diagnoses and biomarkers and overlap, interact, or co-occur in patients with MDD at the individual level [8, 9].

Attempts to categorize depression by matching symptoms to biological underpinnings have emerged in recent years. For example, identified by whole-exome genotyping data, individuals with MDD of the latent genetic subtype have increased common genetic substrates related to the disorder, suffer from paranoid symptoms, and have more anxiety and less sleep maintenance insomnia [10]. The promise of distinguishing depression subtypes in relation to differing patterns of dysfunctional brain connectivity and identifying distinct clinical-symptom profiles to tailor treatments to the individual's specific underlying pathophysiology is compelling [5]. Recent studies have elucidated that brain connectivity-based biotypes of depression fit with diagnostic boundaries [11, 12]. In MDD, there is a possibility that putative biotypes of neural circuit dysfunction may be mapped onto the profiles of symptoms [6, 9]. Despite such promising findings from genetics in relation to functional connectivity, studies exploring biotypes of MDD based on the microstructural abnormalities in the white matter connections are limited.

Techniques using diffusion tensor imaging (DTI) and Tract-Based Spatial Statistics (TBSS) have been developed to obtain microstructural measures of white-matter tracts *in vivo* [13, 14]. With DTI, fractional anisotropy (FA) is the most commonly used metric for measuring the directionality of local water diffusion, which reflects the degree of membrane integrity and myelin thickness, with decreased FA being considered to be related to the disruption of white matter integrity [15]. FA abnormalities occurring in the fiber tracts of individuals with major depression may indicate microstructural changes underlying the pathophysiology of the disorder. This is supported by DTI studies of patients with depression that report impaired white-matter integrity of fiber tracts that contribute to emotional regulation, including the corpus callosum (CC), superior longitudinal fasciculus (SLF), uncinate fasciculus, anterior corona radiata, cingulum, and inferior fronto-occipital fasciculus (IFOF) [16–19].

In the current study we aimed to characterize the diffusion properties of major white-matter tracts using DTI, and to identify potential biotypes of major depression based on the pattern of microstructural alterations. Moreover, we further compared the clinical and neurocognitive

differences between the identified biotypes to parse the heterogeneity underlying the MDD disease mechanisms.

Materials and Methods

Participants

This study recruited 234 right-handed participants, including 116 patients with MDD (72 females; mean age 26.13 years) and 118 demographically-matched healthy control individuals (71 females; mean age 26.01 years). All were Han Chinese between the ages of 16 and 46 years. Inclusion and exclusion criteria are described in the Supplementary material. Diagnosis was based on the Structured Clinical Interview for DSM-IV, and clinical symptoms were assessed using the 17-item Hamilton Rating Scale for Depression (HAM-D) and the 17-item Hamilton Rating Scale for Anxiety (HAM-A). Written informed consent was given by all participants after the study procedure had been fully explained. Ethical approval for this study was granted by the Ethics Committee of the West China Hospital, Sichuan University, in accord with the Declaration of Helsinki.

Neuropsychological Assessments

General intelligence was evaluated at initial assessment using the short version of the Wechsler Adult Intelligence Scale-Revised in China (WAIS-RC) [20]. The 7 subtests of the WAIS-RC were information, arithmetic, digital symbol, digital span test, block design, picture completion, and similarities.

The two subtests of the Cambridge Neuropsychological Test Automated Battery (CANTAB) were the Rapid Visual Information Processing (RVP) for sustained attention and inhibition, and the Delayed Matching to Sample (DMS) for simultaneous and delayed visual memory [21, 22]. The variables of interest across tasks were reaction time, accuracy, and errors (see Table S1).

Magnetic Resonance Imaging Acquisition and Preprocessing

All magnetic resonance imaging (MRI) scans were performed using a Philips 3T scanner (Achieva TX, Best, the Netherlands) and DTI data were acquired from each participant (see scanning parameters in Supplementary Material). Quality control of the DTI data was managed using DTIPrep (translation <2 mm, rotation <0.5 mm) [23]. DTI data were processed using FSL software (FMRIB Software Library, Oxford, UK), including motion and eddy-current correction, brain extraction, tensor model

fitting and MNI normalization of TBSS [24]. Twenty white-matter tracts (listed in the Supplementary Material) identified with the Johns Hopkins University white-matter tractography atlas - were used to delineate convoluted trajectories and relationships with other brain structures in each participant's brain [25, 26].

Feature Extraction, Hierarchical Clustering, and Cluster Validation

After tract identification, FA was computed for each tract and each participant. Hierarchical clustering was performed on the data from patients with MDD using the FA values extracted from the 20 fiber bundles of these tracts. At the individual level, the FA value of each fiber tract was scaled between -1 and 1 before analysis in the clustering procedure. Hierarchical clustering analysis was performed with average linkage and the Euclidean distance to reveal close relationships among the 20 major fiber tracts. The dendrogram illustrates how each cluster is composed by drawing a U-shaped link between a non-singleton cluster and its sub-nodes. In this study, the rescaling (MinMaxScaler) and hierarchical clustering were done with scikit-learn (machine learning in Python: <http://scikit-learn.org/stable/index.html>). In cluster validation, the gap value was adopted to assist in determining the optimal cluster number in the dendrogram (see details of cluster validation in Supplementary Material). According to the definition of the validating metric used, the optimal number of clusters has the largest gap value (see Fig. S1).

Statistical Analysis

After identifying the biotypes of MDD, we first compared the demographic characteristics, including age, sex, and years of education, of each subgroup of MDD patients with healthy controls using the independent two-sample *t*-test and the χ^2 test when appropriate. Moreover, analysis of variance (ANOVA) was used to compare total illness duration and symptom severity (total HAM-D and HAM-A scores) between patient subgroups. The FAs of average identified fiber tracts were compared between healthy controls and patient subgroups with depression using ANOVA. *Post hoc* tests were conducted between patient subgroups and healthy controls. Finally, the General Linear Model (GLM) was used to compare neurocognitive performance in each patient subgroup with the healthy controls, with age, sex, and educational years as covariates. Statistical significance was accepted when the Dunn-Sidak corrected *P* value was <0.05 [27].

Voxel-wise inter-group comparisons (i.e., each patient subgroup *vs* healthy controls) of the skeletonized FA maps were made using *randomize* from FSL [28]. Per contrast,

5000 permutations were conducted with age, sex and years of education as covariates in the model. Threshold-free cluster enhancement (TFCE) was used for multiple testing correction (corrected at $P < 0.05$). See details of TBSS in the Supplementary Material.

In each patient subgroup, the partial correlation was calculated between the average FAs of identified fiber tracts and symptom severity (total scores of HAM-D and HAM-A), and between average FAs and measures of neurocognitive function, with age, sex, and duration of illness as covariates.

Results

Identification of Biotypes Using Hierarchical Clustering

The results of hierarchical clustering are illustrated by the dendrogram and heat map in Fig. 1. From visual inspection, the dendrogram showed three clear clusters. This optimal number of clusters was validated using a clustering validation method, the gap value (see “Materials and Methods” section): the clustering result achieved the maximum gap value when using 3 as the number of clusters. Subsequent analysis primarily focused on these 3 subgroups: subtype 1 with 30 patients (25.9%), subgroup 2 with 50 patients (43.1%), and subgroup 3 with 36 patients (31.0%). Visually, the dendrogram indicated that subgroup 1 had relatively lower FA in most fiber tracts, subgroup 2 had moderate abnormalities, and subgroup 3 had mild alterations.

Each row represents a diffusion property of a fiber tract, and each column represents a patient. Three main subgroups (denoted by subgroups 1, 2, and 3) were identified. FA, fractional anisotropy; L, left; R, right; Fmaj, forceps major; Fmin, forceps minor; ATR, anterior thalamic radiation; CGC, cingulate gyrus of the cingulum; CGH, hippocampal part of the cingulum; CST, corticospinal tract; IFO, inferior fronto-occipital fasciculus; SLf, temporal part of the superior longitudinal fasciculus; UNC, uncinate fasciculus; ILF, inferior longitudinal fasciculus; SLF, superior longitudinal fasciculus.

Demographics and Clinical Symptoms in Patient Subgroups *vs.* Healthy Controls

Table 1 summarizes the demographic and clinical characteristics of the control group and each patient subgroup. Compared to the control group, no significant difference in age, sex, or educational level was found in either subgroup 1 or subgroup 3. Patients in subgroup 2 had a lower educational level than the control group ($T = -2.60$,

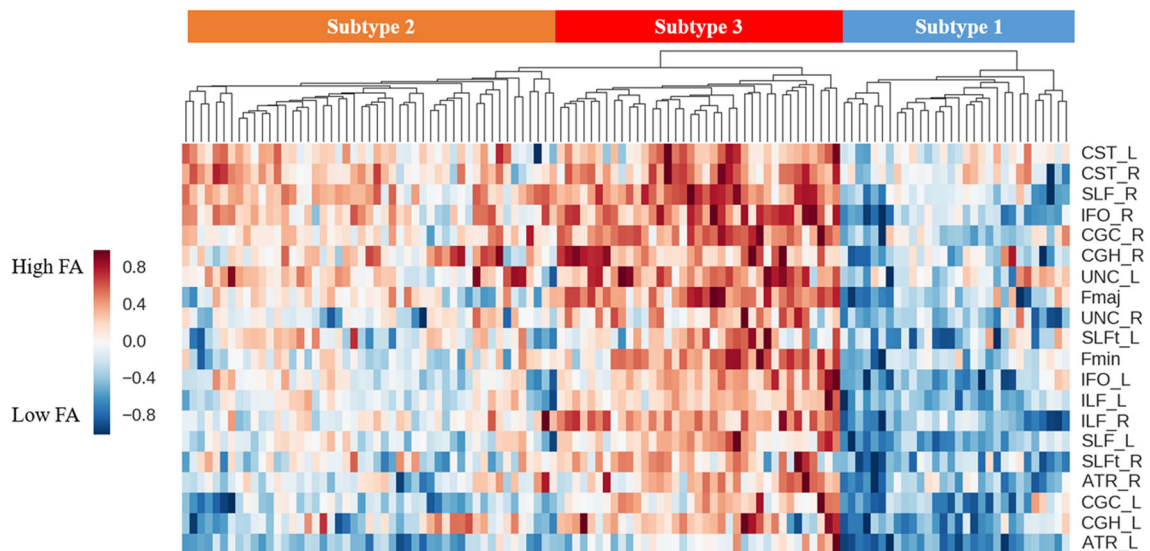


Fig. 1 Dendrogram and heat map illustrating the results of hierarchical clustering.

Table 1 Demographic and clinical characteristics of patient subgroups and control group.

Variable	Subgroup1 (n = 30)	Subgroup2 (n = 50)	Subgroup3 (n = 36)	Healthy controls (n = 118)
<i>Demographic characteristic</i>				
Age, mean (SD)	23.80 (7.25)	27.22 (7.80)	26.56 (6.34)	26.01 (7.24)
Sex, male/female	11/19	15/35	18/18	47/71
Education years, mean (SD)	13.63 (2.65)	12.70 (3.33)^{b*}	14.47 (2.90)	14.12 (3.20)
<i>Clinical characteristics</i>				
Total illness duration, months	25.00 (33.23)	32.93 (59.28)	23.85 (42.06)	NA
Presence of suicidal thoughts, yes/no	15/15	27/23	22/14	NA
Presence of suicidal behavior, yes/no	6/24	5/45	2/34	NA
With/without family history	5/25	5/45	2/34	NA
First episode, yes/no	18/12	30/20	23/13	NA
No medication	24	39	22	NA
<i>Antidepressants (taken at least 3 months ago)</i>				
SSRI/SNRI/NaSSAs	5/1/0	4/5/2	9/4/1	NA
HAM-D, mean (SD)	23.90 (4.79)	21.56 (4.39)	22.47 (4.01)	NA
HAM-A, mean (SD)	15.46 (7.70)	16.65 (7.10)	14.62 (5.78)	NA

NA, not available; HAM-D, Hamilton Rating Scale for Depression; HAM-A, Hamilton Rating Scale for Anxiety; SSRIs, selective serotonin reuptake inhibitors; SNRIs, serotonin–norepinephrine reuptake inhibitors; NaSSAs, noradrenergic and specific serotonergic antidepressants.

^{b*}Subgroup 2 compared to healthy controls, $P < 0.05$.

$P = 0.030$), but showed no significant differences in age or sex. The results of ANOVA did not reveal any statistical differences in either total illness duration, total HAM-D scores, or total HAM-A scores for patients across these three subgroups.

Neurocognitive Function in Patient Subgroups vs. Healthy Controls

There were no significant differences for patient subgroups versus the control group in verbal IQ, performance IQ, or full-scale IQ, while controlling for age, sex, and educational level as covariates (see Table 2).

Subgroup 1. In the RVP task, compared to healthy controls, patients of subgroup 1 had more total false

Table 2 Comparison of neurocognitive test results between controls and patient subgroups.

	Subgroup1	Subgroup2	Subgroup3	HC
<i>IQ</i>				
Verbal IQ	106.77 (13.73)	107.56 (15.29)	106.35 (15.96)	111.97 (15.69)
Performance IQ	103.81 (13.89)	102.51 (15.11)	102.83 (12.54)	109.43 (14.08)
Full scale IQ	106.04 (12.94)	105.83 (14.66)	105.38 (14.39)	111.99 (14.96)
<i>RVP</i>				
RVP_TH	15.93 (6.38)	16.04 (6.47)	16.50 (5.85)	17.16 (6.66)
RVP_TM	9.25 (5.31)	8.92 (5.20)	10.50 (5.85)	8.54 (5.68)
RVP_TFA	4.53 (5.97) ^{a*}	2.22 (2.55)	1.53 (2.66)	2.28 (3.92)
RVP_TCR	228.64 (65.83)	229.88 (68.66)	249.50 (13.06)	238.25 (57.95)
RVP_ML	396.90 (176.63)	413.85 (173.16)	419.60 (97.53)	397.47 (149.58)
<i>DMS</i>				
DMS_MCL	3302.46 (862.46)	3806.51 (1037.83)	3660.62 (1308.04)	3566.87 (895.59)
DMS_MCLA	3417.44 (917.36)	4012.14 (1243.01)	3778.39 (1344.42)	3774.10 (1014.52)
DMS_MCLS	2990.39 (998.33)	3322.36 (1295.71)	3338.51 (1457.27)	3010.15 (809.73)
DMS_TC	33.32 (4.47) ^{a*}	33.86 (4.36) ^{b*}	34.81 (3.51)	35.56 (3.35)
DMS_TCA	23.68 (4.35) ^{a**}	24.14 (4.01) ^{b**}	25.22 (3.50)	25.93 (3.07)
DMS_TCS	9.64 (0.62)	9.71 (0.61)	9.59 (0.56)	9.63 (0.66)
DMS_PEGC	0.18 (0.12) ^{a**}	0.16 (0.12) ^{b**}	0.14 (0.11)	0.11 (0.08)

IQ, intelligence quotient; RVP, rapid visual information processing; DMS, delayed matching to sample; RVP_TFA, total false alarms; DMS_TC, total correct; DMS_TCA, total correct in all delays, DMS_PEGC, probability error given correct. Age, sex and educational level were controlled as covariates in the comparison between each subgroup *versus* the healthy control group (HC). Details of cognitive variables are described in Table S1.

^{a*} $P < 0.05$, ^{a**} $P < 0.01$, subgroup 1 compared to HC, ^{b*} $P < 0.05$, ^{b**} $P < 0.01$, subgroup 2 compared to HC.

alarms as responding outside the response window of a target sequence (*RVP_TFA* $F_{1,137} = 4.79$, $P = 0.03$), which suggested that these patients suffered more deficits in sustained attention and inhibition. In the DMS task, patients of subgroup1 and healthy controls differed significantly in *DMS_TC* ($F_{1,137} = 6.19$, $P = 0.014$), *DMS_TCA* ($F_{1,137} = 7.54$, $P = 0.007$) and *DMS_PEGC* ($F_{1,137} = 7.88$, $P = 0.006$). These patients had more errors in the delayed trials (*DMS_TC*, and *DMS_TCA*), and a higher probability of errors occurring when the previous trial was responded to correctly (*DMS_PEGC*), which suggested that patients in subgroup 1 had more impairment in delayed visual memory.

Subgroup 2. Relative to healthy controls, patients in subgroup 2 experienced more errors on the delayed trials (*DMS_TC* $F_{1,155} = 5.18$, $P = 0.024$, and *DMS_TCA* $F_{1,155} = 7.22$, $P = 0.008$) and a higher probability of errors when the previous trial had a correct response (*DMS_PEGC* $F_{1,155} = 7.25$, $P = 0.008$), which suggested that these patients suffered more deficits in delayed visual memory. No significant differences were found between subgroup 2 and the control group in the RVP task.

Subgroup 3. Patients in subgroup 3 exhibited no statistically significant differences from healthy controls in the

RVP and DMS tasks. This suggested that patients in this subgroup had mild alterations in sustained attention and delayed memory (Fig. 2).

The General Linear Model was used to compare neurocognitive performance between each patient subgroup and healthy controls with age, sex, and educational years as covariates. $*P < 0.05$. $**P < 0.005$. **A** Subgroup 1 had more total false alarms (*RVP_TFA*) in the Rapid Visual Information Processing (RVP) task. **B** Subgroups 1 and 2 had a higher probability of errors when the previous trial had a correct response (*DMS_PEGC*) in the Delayed Matching to Sample (DMS) task. **C** Subgroups 1 and 2 had more errors in the total trials (*DMS_TC*). **D** Subgroups 1 and 2 had more errors in the delayed trials (*DMS_TCA*).

Subgroup Differences in White-Matter Abnormalities

Subgroup 1. Subgroup 1 showed significant widespread reductions in FA relative to the control group in the following tracts: bilateral cingulum hippocampus, CC, bilateral SLF, bilateral internal capsule, bilateral posterior thalamic radiation, superior portion of the bilateral cortical spinal tract (CST), as well as bilateral uncinate fasciculus

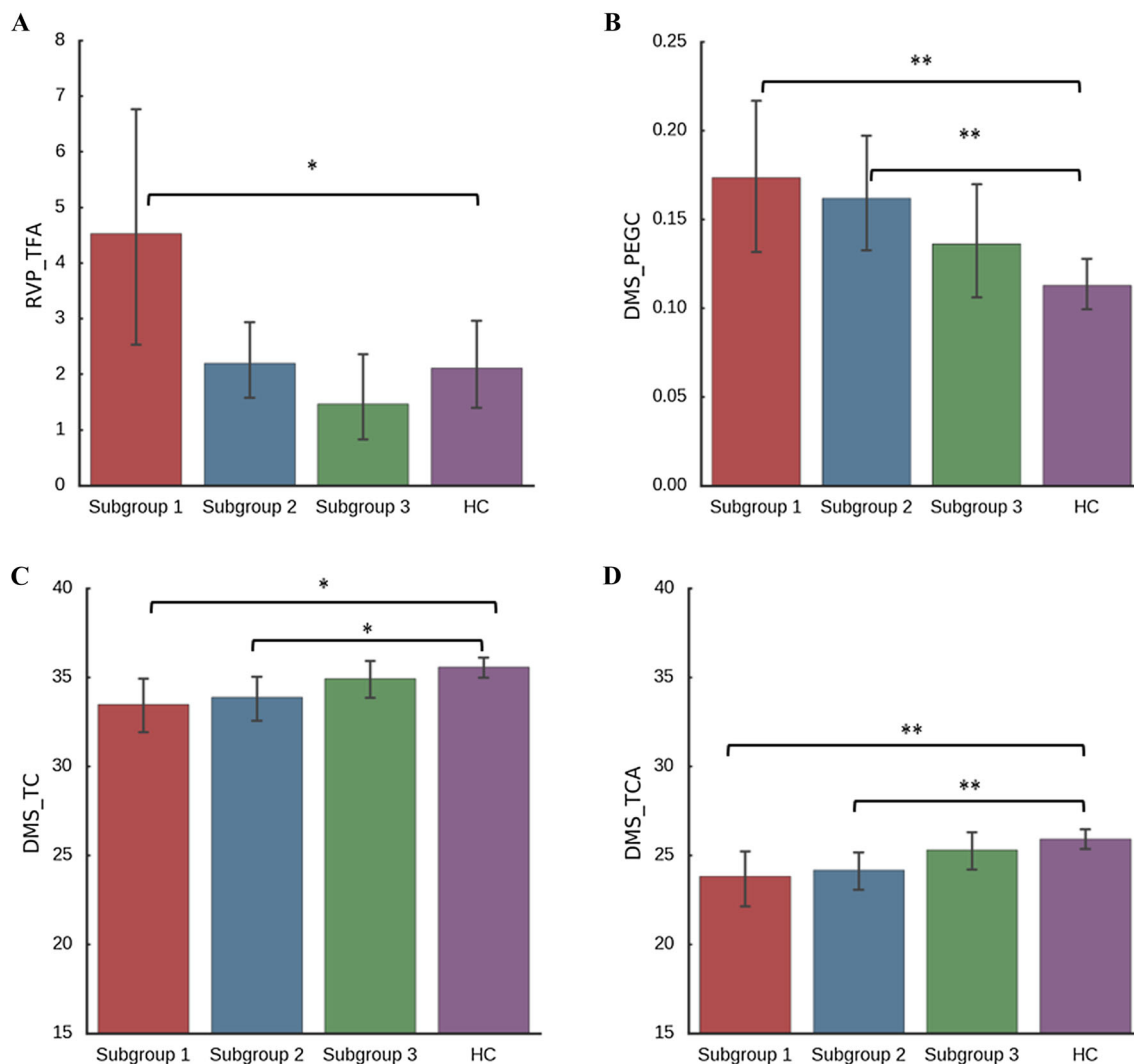


Fig. 2 Neurocognitive function in the patient subgroup *versus* the control group.

and bilateral inferior longitudinal fasciculus (ILF), and bilateral IFOF (Fig. 3 and Fig. S2).

Subgroup 2. Subgroup 2 had regional FA reduction relative to the control group primarily in part of the genu and body of the CC, a small part of the splenium of the CC, a portion of the left cingulum cingulate (gyrus part), and part of the left ILF.

Subgroup 3. No significant disruptions of fiber tracts were found in subgroup 3 relative to the control group, using TFCE family-wise error correction.

Differences Between Subgroups in White-Matter Abnormalities

Compared to subgroup 2, subgroup 1 had widespread white-matter disruptions including most portions of the CC, bilateral SLF, cingulum hippocampus, CST, ILF, right

cingulate gyrus, left IFOF, and anterior thalamic radiation (Fig. S3A). Compared to subgroup 3, subgroup 2 tended to have regional white-matter alterations in a portion of the right CC (Fig. S3B). However, there was no statistically significant difference between subgroups 2 and 3 after the TFCE correction.

The comparisons of average FA between the control group and patient subgroups across 20 fiber tracts are shown in Table S2. Compared to healthy controls, subgroups 1 and 2 had almost the same alterations as the above results. Subgroup 3 had regional FA reduction in the bilateral gyrus part of the cingulum cingulate, and right temporal part of the SLF. Compared to subgroup 2, subgroup 1 had widespread white-matter alterations as above. Subgroup 2 relative to subgroup 3 had FA reduction in the forceps major and the frontal projection of the CC (Fmin), and bilateral of SLF, ILF, and gyrus part of the cingulum cingulate.

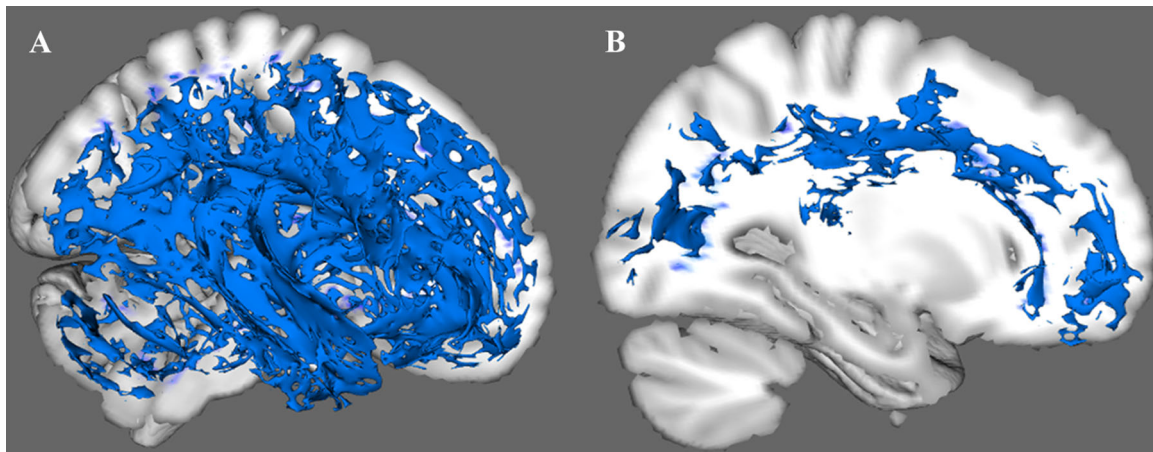


Fig. 3 Patterns of white matter alterations in the patient subgroup *versus* the control group. **A** Subgroup 1 had widespread white-matter abnormalities. **B** Subgroup 2 had regional white-matter alterations,

mainly in a portion of the corpus callosum and part of the left cingulum cingulate.

Partial Correlation Analysis

In each patient subgroup, no significant correlation was found between the average FA of fiber tracts and HAM-A/HAM-D total scores.

In subgroups 1 and 2, the mean FA of the left anterior thalamic radiation was positively correlated with the total correct trails in DMS (DMS_TC , $r = 0.453$, $P = 0.039$). In subgroup 3, the mean FA of the right SLF was positively correlated with total correct trails (DMS_TC , $r = 0.404$, $P = 0.027$) and correct trials in all delays of DMS (DMS_TC_A , $r = 0.368$, $P = 0.045$). In subgroup 3, the mean FA of the right SLF was negatively correlated with the probability of errors given a prior correct trial (DMS_PEGC , $r = -0.366$, $P = 0.047$), and the mean FA of the left gyrus part of the cingulum cingulate was negatively correlated with total false alarms in the RVP task (RVP_TFA , $r = -0.378$, $P = 0.040$).

Discussion

Using a neuroimaging data-driven approach, this study identified three subgroups of patients with MDD by white-matter abnormalities. One pattern revealed a widespread reduction of FA across the fiber tracts; a second pattern indicated regional FA reduction, mainly in aspects of the CC, the left gyrus part of the cingulum cingulate, and part of the left ILF; and the third pattern had no statistically significant alterations in fiber tracts and no significant differences from healthy controls. Although patients in the three subgroups showed no statistical differences in clinical characteristics, including total illness duration and symptom severity of depression and anxiety, each subgroup showed distinct neurocognitive deficits. In brief, subgroup

1 suffered more deficits in sustained attention, inhibition, and delayed visual memory; subgroup 2 had impairment in delayed memory; and subgroup 3 had no statistically significant neurocognitive dysfunction. The current results highlight the potential biological subtypes of individuals with MDD defined by structural connectivity, which could help understand the heterogeneity of the disorder and promote type-specific treatments for potential depressive subtypes.

A prior DTI study reported abnormalities in white-matter pathways, mostly notably in the CC and SLF, and the increased depressive symptom severity was negatively associated with the decreased white-matter integrity [17]. In addition, microstructure abnormalities of the uncinate, IFOF, and CST have been associated with persistent depressive disorder, which elucidated that altered white-matter microstructure in early onset depression might contribute to the maintenance and recurrence of symptoms [18]. Moreover, abnormalities in the genu of the CC detected in the early onset of major depression could persist into adulthood [29]. The disorganization of white matter in the frontal gyrus, parietal lobe, and occipito-temporal gyrus could actually be present early in the course of MDD; this might disrupt the neural circuits involved in mood regulation and thus contribute to the neuropathology of the disorder [30]. In the current study, although no significant differences were found between the three subgroups in the severity of depressive symptoms, individuals in subgroup 1 suffered more neurocognitive deficits in sustained attention, inhibition, and delayed memory, which could be associated with the widespread alterations of white-matter integrity.

MDD is associated with dysfunctions in attention, memory, and executive function, which occur not only in the acute phase of illness but probably persist in phases of

remission [31–33]. Neuroimaging studies have reported that microstructural abnormalities in the anterior CC are associated with the impairments of working memory and sustained attention in patients with major depression [34]. In addition, anomalies of the middle-anterior and middle-posterior cingulum bundle, major links within the limbic-cortical networks, are related to executive function and divided attention in depressed individuals [35]. Besides, previous animal studies have indicated that impaired learning and memory involve increased brain cytokine signaling in response to peripheral immune activation, which might increase the risk of major depressive episodes [36]. Moreover, the increased miR-132 in major depression is related to the dysfunction of fronto-limbic areas and linked to the relevant neurocognitive deficits in attention and executive function. Furthermore, the genes affecting mitochondrial functions could contribute to the phenotype of depression characterized by accompanying neurocognitive impairments [37]. From this study, the three subgroups with the varying degrees of neurocognitive deficits corresponding to different patterns of white-matter alterations could be used as a potential basis for differentiating between different phenotypes of MDD.

Factors such as epigenetic regulatory processes and signal transduction also affect the structural integrity in individuals with major depression. The white-matter integrity of the CC (body) is significantly associated with elevated DNA methylation of the serotonin transporter gene *SLC6A4*, suggesting potential modulatory effects of gene-environment interactions on the structural integrity of the white matter in depression [38]. In addition, methylation of the brain-derived neurotrophic factor promoter region is related to the integrity of the anterior corona radiata, that may contribute to the structural white-matter changes in individuals with major depression [39]. Moreover, a postmortem study revealed that the significant differences in the methylation patterns were specific to astrocytic dysfunction associated with depressive psychopathology [40]. DNA methylation, as the most stable epigenetic marker, may be triggered by the environmental stress and potentially lead to vulnerability to depression [41]. Furthermore, cell communication and signal transduction mechanisms might contribute to oligodendroglial and synaptic abnormalities in the temporal cortex of patients with major depression [42]. In the current study, the identified three subgroups with distinct white-matter patterns of major depression which may, to some extent, have quantitatively or qualitatively different biological underpinnings, particularly in epigenetics.

In recent years, functional neuroimaging has proven its utility in clustering individuals according to shared features of brain dysfunction in participants with major depression [5]. The data-driven parsing of neural connectivity reveals

the heterogeneous underpinnings of depression subgroups with unique neural connectivity profiles and co-occurring clinical symptoms [6]. Besides, the disease duration and symptom severity might dominate the parsing of functional connectivity among depression-related brain regions at the individual level [12]. Subgroups with identified distinct functional connectivity during positive mood induction could provide clinically relevant information (symptom severity) that is evident across symptoms, affect, and behavior and that might be a discrete marker of neurobiology [11]. Clustering findings in the functional and structural connectivity of depression provide a plausible biological basis for the neuroimaging biological subtypes reported in previous studies and here. Neuroimaging scans coupled with machine learning algorithms as reported in the current study may be involved in stratifying patients with major depression into biological subtypes – eventually translating into individual patient-tailored therapeutic interventions.

Possible study limitations should be considered. First, the sample size of the current study was moderate, with relatively small sample sizes in each patient subgroup. Replication studies, especially with larger and independent samples, are needed to validate the three identified subgroups, to improve the robustness and generalizability of the clustering findings. More measures of brain white-matter should be used to explore the biotypes of major depression in future studies. Second, the current study was based on cross-sectional analysis, but could be combined with a longitudinal follow-up study that may help predict the therapeutic effects and prognosis of the different subgroups, especially the subgroup with widespread white-matter disruptions. Third, it will be fruitful to collect more clinical variables (such as personality characteristics and early life stress), and evaluate both affective and psychotic symptoms in individuals with MDD. When comparing clinical characteristics between subgroups, a multivariate vector should be used to represent clinical scores as a whole, rather than treat them separately. Fourth, although some of the relapsed depressive patients had not taken antidepressants in the preceding three months or more, it is hard to evaluate the influence of previous medication effects.

In conclusion, the current study used a data-driven method to identify three subgroups by a stepwise pattern of white-matter alterations in individuals with MDD. The neurocognitive deficits of each subgroup corresponded with its white-matter disruptions. The subgroup with widespread white-matter abnormalities suffered more deficits in sustained attention, inhibition, and delayed visual memory, suggesting a distinct neurobiologically-based biotype. The results from this study of neurobiological subtypes of MDD (reflected by distinct patterns of

white-matter alterations accompanying relative degrees of neurocognitive deficit) suggests a novel pathway to understanding the heterogeneity of MDD that may lead to the optimization of subtype-specific treatment approaches.

Acknowledgements All participants in the study are most warmly thanked. This work was supported by the National Natural Science Foundation of China (81630030, 81130024, 81801326, and 81571320), the National Natural Science Foundation of China/Research Grants Council of Hong Kong Joint Research Scheme (81461168029), the National Basic Research Development Program of China (2016YFC0904300), the 1.3.5 Project for Disciplines of Excellence, West China Hospital of Sichuan University, the National High-Technology Research and Development Project (863 Project) of China (2015AA020513), and a Scientific Project of Sichuan Science and Technology Department, China (2015JY0173).

Conflict of Interest The authors declare that they have no conflict of interest.

References

1. Organization WH. International statistical classification of diseases and related health problems. World Health Organization, 2004.
2. Association AP. Diagnostic and statistical manual of mental disorders (DSM-5®). American Psychiatric Pub, 2013.
3. Paykel ES. Basic concepts of depression. *Dialogues Clin Neurosci* 2008, 10: 279–289.
4. van Loo HM, de Jonge P, Romeijn JW, Kessler RC, Schoevers RA. Data-driven subtypes of major depressive disorder: a systematic review. *BMC Med* 2012, 10: 156.
5. Drysdale AT, Grosenick L, Downar J, Dunlop K, Mansouri F, Meng Y, *et al.* Erratum: Resting-state connectivity biomarkers define neurophysiological subtypes of depression. *Nat Med* 2017, 23: 264.
6. Price RB, Gates K, Kraynak TE, Thase ME, Siegle GJ. Data-driven subgroups in depression derived from directed functional connectivity paths at rest. *Neuropsychopharmacology* 2017, 42: 2623–2632.
7. Wager TD, Woo CW. Imaging biomarkers and biotypes for depression. *Nat Med* 2017, 23: 16–17.
8. Song M, Yang Z, Sui J, Jiang T. Biological subtypes bridge diagnoses and biomarkers: a novel research track for mental disorders. *Neurosci Bull* 2017, 33: 351–353.
9. Williams LM. Precision psychiatry: a neural circuit taxonomy for depression and anxiety. *Lancet Psychiatry* 2016, 3: 472–480.
10. Yu C, Arcos-Burgos M, Licinio J, Wong ML. A latent genetic subtype of major depression identified by whole-exome genotyping data in a Mexican-American cohort. *Transl Psychiatry* 2017, 7: e1134.
11. Price RB, Lane S, Gates K, Kraynak TE, Horner MS, Thase ME, *et al.* Parsing heterogeneity in the brain connectivity of depressed and healthy adults during positive mood. *Biol Psychiatry* 2017, 81: 347–357.
12. Feder S, Sundermann B, Wersching H, Teuber A, Kugel H, Teismann H, *et al.* Sample heterogeneity in unipolar depression as assessed by functional connectivity analyses is dominated by general disease effects. *J Affect Disord* 2017, 222: 79–87.
13. Le Bihan D, Mangin JF, Poupon C, Clark CA, Pappata S, Molko N, *et al.* Diffusion tensor imaging: concepts and applications. *J Magn Reson Imaging* 2001, 13: 534–546.
14. Smith SM, Jenkinson M, Johansen-Berg H, Rueckert D, Nichols TE, Mackay CE, *et al.* Tract-based spatial statistics: voxelwise analysis of multi-subject diffusion data. *Neuroimage* 2006, 31: 1487–1505.
15. Winston GP. The physical and biological basis of quantitative parameters derived from diffusion MRI. *Quant Imaging Med Surg* 2012, 2: 254–265.
16. Kieseppa T, Eerola M, Mantyla R, Neuvonen T, Poutanen VP, Luoma K, *et al.* Major depressive disorder and white matter abnormalities: a diffusion tensor imaging study with tract-based spatial statistics. *J Affect Disord* 2010, 120: 240–244.
17. Cole J, Chaddock CA, Farmer AE, Aitchison KJ, Simmons A, McGuffin P, *et al.* White matter abnormalities and illness severity in major depressive disorder. *Br J Psychiatry* 2012, 201: 33–39.
18. Vilgis V, Vance A, Cunningham R, Silk TJ. White matter microstructure in boys with persistent depressive disorder. *J Affect Disord* 2017, 221: 11–16.
19. Jiang J, Zhao YJ, Hu XY, Du MY, Chen ZQ, Wu M, *et al.* Microstructural brain abnormalities in medication-free patients with major depressive disorder: a systematic review and meta-analysis of diffusion tensor imaging. *J Psychiatry Neurosci* 2017, 42: 150–163.
20. Gong Y. Wechsler adult intelligence scale-revised in China Version. Hunan Medical College, Changsha, Hunan/China 1992.
21. Sahakian B, Owen A. Computerized assessment in neuropsychiatry using CANTAB: discussion paper. *J R Soc Med* 1992, 85: 399–402.
22. Maric NP, Stojanovic Z, Andric S, Soldatovic I, Dolic M, Spiric Z. The acute and medium-term effects of treatment with electroconvulsive therapy on memory in patients with major depressive disorder. *Psychol Med* 2016, 46: 797–806.
23. Oguz I, Farzinfar M, Matsui J, Budin F, Liu Z, Gerig G, *et al.* DTIPrep: quality control of diffusion-weighted images. *Front Neuroinform* 2014, 8: 4.
24. Jenkinson M, Beckmann CF, Behrens TE, Woolrich MW, Smith SM. FSL. *Neuroimage* 2012, 62: 782–790.
25. Mori S, Oishi K, Faria AV. White matter atlases based on diffusion tensor imaging. *Curr Opin Neurol* 2009, 22: 362–369.
26. Wakana S, Caprihan A, Panzenboeck MM, Fallon JH, Perry M, Gollub RL, *et al.* Reproducibility of quantitative tractography methods applied to cerebral white matter. *Neuroimage* 2007, 36: 630–644.
27. Sidak Z. Rectangular confidence regions for the means of multivariate normal distributions. *J Am Stat Assoc* 1967, 62: 626–633.
28. Winkler AM, Ridgway GR, Webster MA, Smith SM, Nichols TE. Permutation inference for the general linear model. *Neuroimage* 2014, 92: 381–397.
29. Kemp A, MacMaster FP, Jaworska N, Yang XR, Pradhan S, Mahnke D, *et al.* Age of onset and corpus callosal morphology in major depression. *J Affect Disord* 2013, 150: 703–706.
30. Ma N, Li L, Shu N, Liu J, Gong G, He Z, *et al.* White matter abnormalities in first-episode, treatment-naive young adults with major depressive disorder. *Am J Psychiatry* 2007, 164: 823–826.
31. Snyder HR. Major depressive disorder is associated with broad impairments on neuropsychological measures of executive function: a meta-analysis and review. *Psychol Bull* 2013, 139: 81–132.
32. Hammar A, Ardal G. Cognitive functioning in major depression—a summary. *Front Hum Neurosci* 2009, 3: 26.
33. Liang S, Vega R, Kong X, Deng W, Wang Q, Ma X, *et al.* Neurocognitive graphs of first-episode schizophrenia and major depression based on cognitive features. *Neurosci Bull* 2018, 34: 312–320.
34. Yamada S, Takahashi S, Ukai S, Tsuji T, Iwatani J, Tsuda K, *et al.* Microstructural abnormalities in anterior callosal fibers and

- their relationship with cognitive function in major depressive disorder and bipolar disorder: a tract-specific analysis study. *J Affect Disord* 2015, 174: 542–548.
35. Schermuly I, Fellgiebel A, Wagner S, Yakushev I, Stoeter P, Schmitt R, *et al.* Association between cingulum bundle structure and cognitive performance: an observational study in major depression. *Eur Psychiatry* 2010, 25: 355–360.
 36. Dantzer R, O'Connor JC, Freund GG, Johnson RW, Kelley KW. From inflammation to sickness and depression: when the immune system subjugates the brain. *Nat Rev Neurosci* 2008, 9: 46–56.
 37. Petschner P, Gonda X, Baksa D, Eszlari N, Trivaks M, Juhasz G, *et al.* Genes linking mitochondrial function, cognitive impairment and depression are associated with endophenotypes serving precision medicine. *Neuroscience* 2018, 370: 207–217.
 38. Won E, Choi S, Kang J, Kim A, Han KM, Chang HS, *et al.* Association between reduced white matter integrity in the corpus callosum and serotonin transporter gene DNA methylation in medication-naive patients with major depressive disorder. *Transl Psychiatry* 2016, 6: e866.
 39. Choi S, Han KM, Won E, Yoon BJ, Lee MS, Ham BJ. Association of brain-derived neurotrophic factor DNA methylation and reduced white matter integrity in the anterior corona radiata in major depression. *J Affect Disord* 2015, 172: 74–80.
 40. Nagy C, Suderman M, Yang J, Szyf M, Mechawar N, Ernst C, *et al.* Astrocytic abnormalities and global DNA methylation patterns in depression and suicide. *Mol Psychiatry* 2015, 20: 320–328.
 41. Booij L, Wang D, Levesque ML, Tremblay RE, Szyf M. Looking beyond the DNA sequence: the relevance of DNA methylation processes for the stress-diathesis model of depression. *Philos Trans R Soc Lond B Biol Sci* 2013, 368: 20120251.
 42. Aston C, Jiang L, Sokolov BP. Transcriptional profiling reveals evidence for signaling and oligodendroglial abnormalities in the temporal cortex from patients with major depressive disorder. *Mol Psychiatry* 2005, 10: 309–322.